

Communication

Cytomorphological Characterization of Individual Metastatic Tumor Cells from Gastrointestinal Cancer Patient Lymph Nodes with Imaging Flow Cytometry

Marnie Winter ¹, Rachel Gibson ², Andrew Ruzskiewicz ³ and Benjamin Thierry ^{1,*}

¹ Future Industries Institute and ARC Centre of Excellence in Convergent Bio-Nano Science and Technology, University of South Australia, Adelaide 5095, Australia; marnie.winter@mymail.unisa.edu.au

² Faculty of Health and Medical Sciences, University of Adelaide, Adelaide 5000, Australia; rachel.gibson@adelaide.edu.au

³ Department of Surgical Pathology, SA Pathology, Centre for Cancer Biology, University of South Australia, Adelaide 5000, Australia; andrew.ruzskiewicz@sa.gov.au

* Correspondence: Benjamin.Thierry@unisa.edu.au; Tel.: +61-8-8302-368

Received: 16 July 2019; Accepted: 19 September 2019; Published: 26 September 2019



Abstract: The presence or absence of tumor cells within patient lymph nodes is an important prognostic indicator in a number of cancer types and an essential element of the staging process. However, patients with the same pathological stage will not necessarily have the same outcome. Therefore, additional factors may aid in identifying patients at a greater risk of developing metastasis. In this proof of principle study, initially, spiked tumor cells in rat lymph nodes were used to mimic a node with a small cancer deposit. Next, human lymph nodes were obtained from cancer patients for morphological characterization. Nodes were dissociated with a manual tissue homogenizer and stained with fluorescent antibodies against CD45 and Pan-Cytokeratin and then imaging flow cytometry (AMNIS ImageStreamX Mark II) was performed. We show here that imaging flow cytometry can be used for the detection and characterization of small numbers of cancer cells in lymph nodes and we also demonstrate the phenotypical and morphological characterization of cancer cells in gastrointestinal cancer patient lymph nodes. When used in addition to conventional histological techniques, this high throughput detection of tumor cells in lymph nodes may offer additional information assisting in the staging process with therapeutic and prognostic applications.

Keywords: imaging flow cytometry; lymph node; metastasis; cellular morphology; cancer

1. Introduction

The presence of metastatic cancer cells within regional lymph nodes, including in sentinel lymph nodes (SLNs), is a significant prognostic indicator in a number of cancer types including gastrointestinal (GI) cancers [1]. Importantly, positive identification of metastatic tumor cells in lymph nodes may indicate the need for adjuvant therapy [2]. The size of cancer deposits in lymph nodes is also clinically relevant. These can be defined as either (1): Macrometastasis (>2 mm), (2): Micrometastasis (0.2–2 mm), or (3): Isolated tumor cells (ITCs; <0.2 mm) [1]. Prognostic significance for the smaller deposits (including micrometastasis and ITC) is highly debated and is likely to vary between cancer types [3–7]. Determining which patients with positive nodes require Axillary Lymph Node Dissection (ALND) and that would benefit from adjuvant radiotherapy and systemic treatment is a problem [8] as some lymph node metastasis may never develop into clinically detectable disease [9]. Therefore, additional approaches to identify individuals with a higher likelihood of developing metastatic disease are required to provide better prognostication and selection for adjuvant treatment [10].

Currently, lymph node involvement by tumor is assessed using histological methods which may be complemented by immunohistochemical (IHC) analysis of formalin fixed paraffin embedded (FFPE) tissue postoperatively or frozen sections intra-operatively [11]. Increasing the number of sections examined of the resected node analyzed, accompanied with the use of targeted molecular methods increases small deposit detection [1]; however, these methods are not routinely used in the pathological practice as their reliability to detect small deposits is questioned [12]. Advances for disseminated tumor cell (DTC) detection in lymph nodes have primarily focused on increasing sensitivity of detection and increasing speed of diagnosis. DTC include cancer cells that leave the primary tumor via the lymphatics and can lodge in lymph nodes and go on to form a metastatic deposit. To date, individual tumor cell morphology following isolation from lymph nodes has not been investigated, despite the fact it could provide clinically important information. Conversely, a very intensive research effort has been undertaken in recent years to elucidate the clinical significance of circulating tumor cells (CTCs) [13–15] and plasma circulating tumor DNA (ctDNA) in peripheral blood [16]. Recent advances in molecular analysis of ctDNA with next generation sequencing and advanced computational analysis allows for tumor genotyping and has demonstrated clinically relevant mutational analysis [16].

Importantly, the isolation and characterization of CTCs is a very active research topic providing clinically relevant information on the metastatic progression of disease in a number of human cancers [13–15]. The main advantage of assessing CTCs and ctDNA is the ease of blood sample acquisition (liquid biopsies) at multiple time points in contrast to invasive procedures required to collect tumor tissue. With the advent of advanced isolation technologies, individual cellular morphological characterization of cancer cells and the importance of morphology for correlation with patient prognosis has been investigated [17–21].

The aims of the current study were to demonstrate the feasibility of using imaging flow cytometry (IFC) for the cytomorphological detection of tumor cells in lymph nodes. IFC is a technique combining the high throughput quantitative nature of flow cytometry with high resolution imaging. The use of IFC is a rapidly emerging area with a number of studies demonstrating its capabilities and advantages [22–25]. Recently, Doan and colleagues discussed the potential of imaging flow cytometry with a particular focus on promising developments that would make IFC more clinically viable as a diagnostic and prognostic tool, including deep learning and cloud computing [26]. We conducted an initial model study using rat lymph nodes spiked with a small number of cancer cells simulating a model of a lymph node with ITC or micrometastasis. Once the feasibility was demonstrated, we proposed a method to detect and characterize tumor cells from resected GI patient lymph nodes with a focus on detecting potentially relevant cytomorphological alterations including circularity/elongation, which may provide prognostic insights into disease progression (Figure 1).

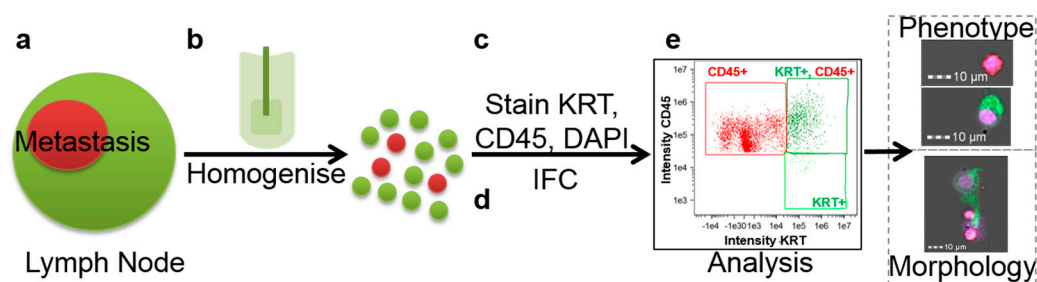


Figure 1. Schematic representation of the experimental design: (a) Lymph nodes are collected and then (b) homogenized with a manual tissue homogenizer; liberated cells were then (c) stained with DAPI to identify the nucleus, Cytokeratin (KRT) to identify epithelial cells and CD45 to identify the lymphoid population. (d) Sample was then run on the imaging flow cytometer (IFC) and then (e) analyzed and characterized based on their phenotype and morphology with brightfield (BF), darkfield (DF), and fluorescence.

2. Materials and Methods

2.1. Spiking Experiments

Human breast adenocarcinoma cell line MCF-7 (ATCC, USA) with a passage number lower than 20 was used in this study to mimic patient metastatic tumor cells and mixed with rat mesenteric lymph nodes. The cancer cell line was cultured in 25 or 75 cm² tissue culture flasks (Sarstedt, Nümbrecht, Germany) in DMEM supplemented with fetal bovine serum (FBS) and penicillin/streptomycin at 37 °C, 5% CO₂ in a humidified environment. Mesenteric rat lymph nodes were scavenged from a study approved by the Animal Ethics Committees of the Institute of Medical and Veterinary Science and The University of Adelaide, and complied with the National Health and Medical Research Council (Australia) Code of Practice for Animal Care in Research and Teaching (2014). Lymph nodes were obtained from the mesentery and separated from the mesenteric fat. All lymph nodes used for spiking experiments were used within 2 days following collection (generally within 24 h) and were stored in RPMI at 4 °C. Each sample constituted approximately 4 lymph nodes weighing approximately 15 mg each (in order to better mimic cellular numbers expected to be recovered from patient samples) and 500 MCF-7 cancer cells were added to the PBS solution prior to homogenization. Lymph nodes without the addition of cancer cells were also processed with the same protocol as a negative control. Cells were stained with fluorescently labeled fluorochromes (Anti-Rat CD45 APC and Anti-Pan-Cytokeratin (KRT)) AE1/AE3 Alexa Fluor® 488 (eBioscience, San Diego, CA, USA) to enable use with the IFC.

2.2. Human Lymph Node

Samples of human lymph nodes were obtained from surgical resections of gastric, colorectal, and gall bladder cancers performed at the Royal Adelaide Hospital, South Australia, surplus to diagnostic requirements. The resection specimens were received fresh and a small portion of nodal tissue not exceeding 20% of node volume was sampled for research. The remaining lymph node tissue was fixed in formalin and examined at multiple levels using the routine pathological method.

The research was carried out according to The Code of Ethics of the World Medical Association (Declaration of Helsinki). All patients gave their written informed consent and the study was approved by the Royal Adelaide Hospital Human Research Ethics Committee and the University of South Australia Human Research Ethics Committee (Protocol Number 130106 and 0000031109). The fresh sample of the lymph node tissue was placed in saline and kept at 4 °C (for less than 3 days) until tissue dissociation and staining. Dissociation and staining of 2 GI cancer patient lymph nodes (one positive, one negative) was included in this feasibility study (Table 1) and allowed for the identification of KRT positive cells in the tested positive node (a node classified as positive for cancerous lesion based on standard H&E staining and observation by a pathologist, as part of their routine care).

Table 1. Cancer patient characteristics.

Patient	1	2	3
Age	55	64	67
Gender	F	M	F
Primary Tumor Site	Stomach	Sigmoid Colon	Gall Bladder
Positive Nodes	29	0	0
Stage	pT3pN3bcM1 Clinical Stage (AJCC) IV	pT2pN0cM0 Clinical Stage (AJCC) I	pT3pN0cM1 Clinical Stage (AJCC) IVB

2.3. Tissue Dissociation

Rat lymph nodes were dissociated whole, while human lymph node tissue was cut into 4 or 5 (depending on size, pieces were approximately 2 mm³) pieces before being dissociated with a manual tissue homogenizer in PBS with 10% FBS (yielding the best cell recovery, Figure S1). The sample was

then filtered through a size 200 mesh with a wire diameter of 0.053 mm and an opening size of 73.7 μm (S4145; Sigma-Aldrich, St. Louis, MO, USA) before undergoing staining.

2.4. Immunofluorescent Cellular Staining

Cellular staining was based on the protocol described by Liu et al. [27]. Briefly after dissociation, cells were washed with 1 \times PBS and non-specific binding was blocked with 10% FBS in basic buffer (1 \times PBS and 0.5% sodium azide) for 15 min on ice. Cells were stained with an Anti-human CD45 antibody (HI30) PE-Cy5.5 (eBioscience, San Diego, CA, USA) for 30 min in basic buffer with 1% FBS and subsequently fixed with 4% formalin fixation solution (Sigma-Aldrich, St. Louis, MO, USA) for 30 min at room temperature. After permeabilization with 0.05% Triton X-100 (Merck Millipore, Bedford, MA, USA), cells were stained with Alexa Fluor[®] 488 Pan-Cytokeratin AE1/AE3 (eBioscience, San Diego, CA, USA), and nuclear stain DAPI (Sigma-Aldrich, St. Louis, MO, USA). Cells were washed with basic buffer and stored with stabilizing fixative (BD Biosciences, San Jose, CA, USA) before analysis with IFC.

2.5. Imaging Flow Cytometry

Following fixation and staining, samples were imaged using an AMNIS[®] ImageStream[®]X Mark II multispectral imaging flow cytometer (Luminex Corporation, Austin, TX, USA), 1 camera system (providing maximum of 6 channels). Events were acquired at 40 \times magnification (60 μm field of view with 0.5 μm per pixel and a 0.75 numerical aperture) using 405 nm laser (DAPI, 100 mW and 40 mW for human and rat experiments, respectively), 488 nm laser (Alexa Fluor[®] 488, PE-Cy5.5, at 100 mW and 65 mW for human and rat experiments, respectively), 642 nm (APC, 150 mW) and 785 nm laser (darkfield/side scatter, 3 mW). Data analysis was performed using IDEAS image-analysis software (Version 6.0; AMNIS, Seattle, WA, USA). A compensation matrix was made with single color control files using the analysis software (Supplementary Tables S1 and S2) and software compensation was performed. Briefly, cells were classified using the following method, in-focus events were selected based on Gradient RMS feature (measures the sharpness of an image by detecting large changes in pixel values), DAPI positive events were then selected to eliminate debris without nuclear staining and then a scatterplot of CD45 PE-Cy5.5 against Cytokeratin Alexa Fluor[®] 488 was produced (Figures 2 and 3). High Cytokeratin and low CD45 and high Cytokeratin and high CD45 events were selected (see Supplementary Information; Figure S4 for more information regarding gating strategy). In order to obtain a single cell population, if required, for morphological analysis, cells were classified based on their brightfield images (including aspect ratio) and keratin expression. After identification of the KRT positive cancer cell population cellular cytomorphology was characterized using the analysis software.

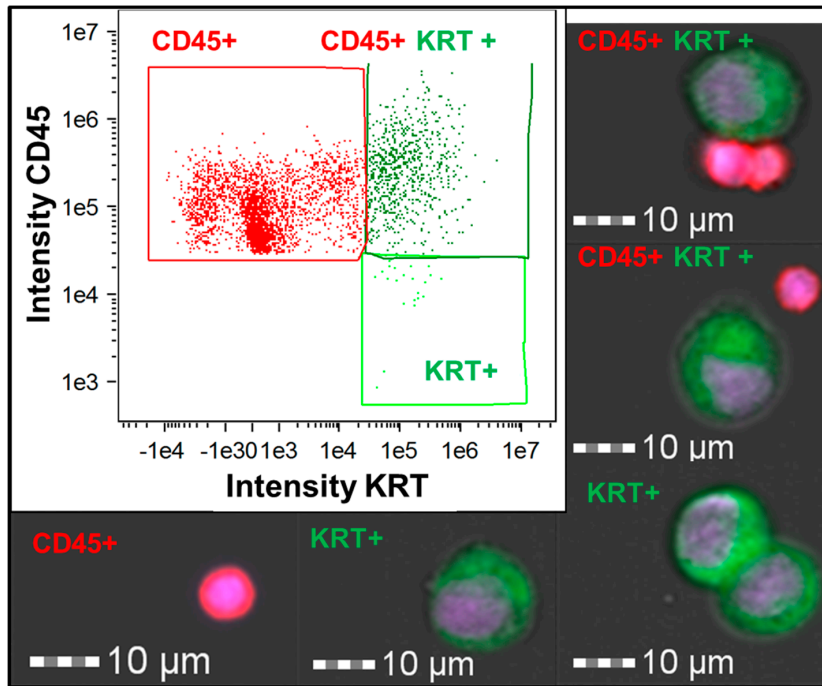


Figure 2. Scatter plot of CD45 against Cytokeratin (KRT) intensity from 50,000 MCF-7 cells spiked into rat lymph nodes with identification of CD45+, KRT+, and double positive KRT+ CD45+ events.

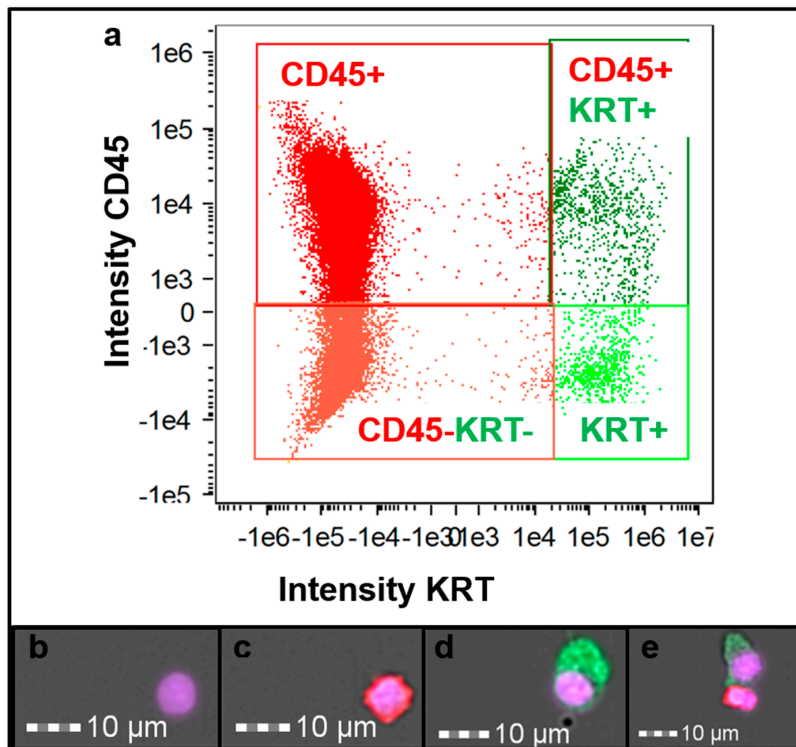


Figure 3. (a) Patient 1 scatter plot of CD45 intensity against Cytokeratin (KRT) intensity, separating white blood cells (WBC; CD45+, 58% gated, mean fluorescence intensity (MFI) CD45 9670) from cancerous cells (KRT+, 0.17% gated), from double positive events (CD45+, KRT+, 0.43% gated, MFI CD45 32,353, KRT 139,167), and double negative events (CD45-, KRT-, 41% gated) found with dissociated human lymph node tissue. (b) CD45- KRT- event most likely a WBC with no CD45 staining. (c) CD45 positive WBC. (d) KRT positive cancer cell from Patient 1. (e) Double positive (KRT, CD45) event containing a WBC and a cancer cell from Patient 1.

3. Results

3.1. Identification and Characterization of Cancer Cells in a Lymph Node Spiking Model

To demonstrate the feasibility of conducting high quality cytomorphological characterization of tumor cells in a lymphoid population using IFC, tumor cells were spiked in rat lymph nodes. IFC was successfully able to detect the cancerous cells among lymphoid cells based on the Cytokeratin (KRT) and CD45 immunostaining (Figure 2). Moreover, IFC detected double positive KRT and CD45 events, once visualized it could be seen that these events contained two or more cells, at least one KRT positive cancer cell and one CD45 positive white blood cells (WBC) (Figure 2). Importantly, these events are very common. As demonstrated in Figure 2, most Cytokeratin positive events were detected as a double positive. Further characterization including morphological analysis could also be performed to help further distinguish these events. No positive events were found in the negative control sample (lymph nodes without spiked cancer cells).

Next, we aimed to demonstrate the feasibility of using IFC to detect small numbers of cancer cells in lymph node tissue to represent the clinical setting where patients may present with ITC or micrometastatic lesions (Figure S2). We were successfully able to detect cancer cells from samples spiked with low numbers (500 cells spiked, 103 cancer cells recovered in a total sample of 230,000 cells) of MCF-7 cancer cells. The recovery yield was calculated to be 20% ($n = 2$) or one in five spiked cells. Quantification of cellular loss during the process was achieved through the recovery and analysis of all supernatants from the staining procedure taken from lymph node spiking experiments. We found approximately 40% ($n = 5$) of the total cellular population was lost during the staining process. Based on this data we expect tumor cells could be recovered and analyzed using the proposed approach even for very small tumor deposits.

3.2. Cancer Patient Lymph Node Analysis

The next aim of the study was to demonstrate the feasibility of detecting and analyzing tumor cells in patients' lymph nodes (Figure 3). A total of 1040 tumor cells (defined as being KRT Alexa Fluor® 488 positive, CD45 PE-Cy5.5 negative and with a DAPI positive nucleus) were recovered from a positive cancer node (Patient 1) (Figure 3d) from approximately 270,000 recorded events. In addition to tumor cells, the vast majority of events were WBC which were characteristically CD45 positive KRT negative (Figure 3c). IFC also identified events which were both KRT and CD45 positive. As noted above, further analysis of these cells showed the presence of two (cancer cells and WBCs) or more cells together; and were classified as one double positive event (Figure 3e). CD45, KRT negative events were also detected (Figure 3b). Conversely, no KRT positive cells were found in the negative control lymph node (Patient 2). However, some events were classified as positive. Morphologically these were subsequently confirmed to be fluorescent bubbles or autofluorescent debris (Supplementary Information, Figure S3).

3.3. Tumor Cell Cytomorphological Characterization

Following IFC further phenotypic analysis showed slight heterogeneous KRT expression of tumor cells in Patient 1 (Figure 4a). The cancer cells also varied in their darkfield (Figure 4b) (side scatter/granularity) and darkfield modulation (Figure 4c). Morphological characterization of these cells was conducted to determine perimeter (Figure 4d), width (Figure 4e), length (Figure 4f), and area (Figure 4g) of KRT (cytoplasmic staining) in Patient 1 as well as DAPI (nuclear area) (Figure 4h). Morphological characterization also demonstrated the KRT positive cell population recovered could be separated into two populations based on their circularity, one classified round and the other classified elongated (Figure 4i). Circularity measures the degree of the events deviation from a circle. Its measurement is based on the average distance of the object boundary from its center divided by the variation of this distance. Thus, the closer the object is to a circle, the smaller the variation and therefore the feature value will be high. Therefore, the more the shape varies from a circle the higher the variation

and the circularity value will be low. The malignant sample had approximately 20% of cells which were classified rounded and 80% classified elongated. For the circularity feature based on image morphology an arbitrary cut off value of 9 was decided upon to distinguish between the two cellular morphologies. Thus, any cells with a circularity value of less than 9 was considered to be elongated (Figure 5b) and anything greater than 9 was considered to be round (Figure 5a). Small un-dissociated KRT positive clumps were also identified in the sample and could be included in enumeration. A small number of KRT events displayed long finger like protrusions and were very elongated (Figure 5b,c).

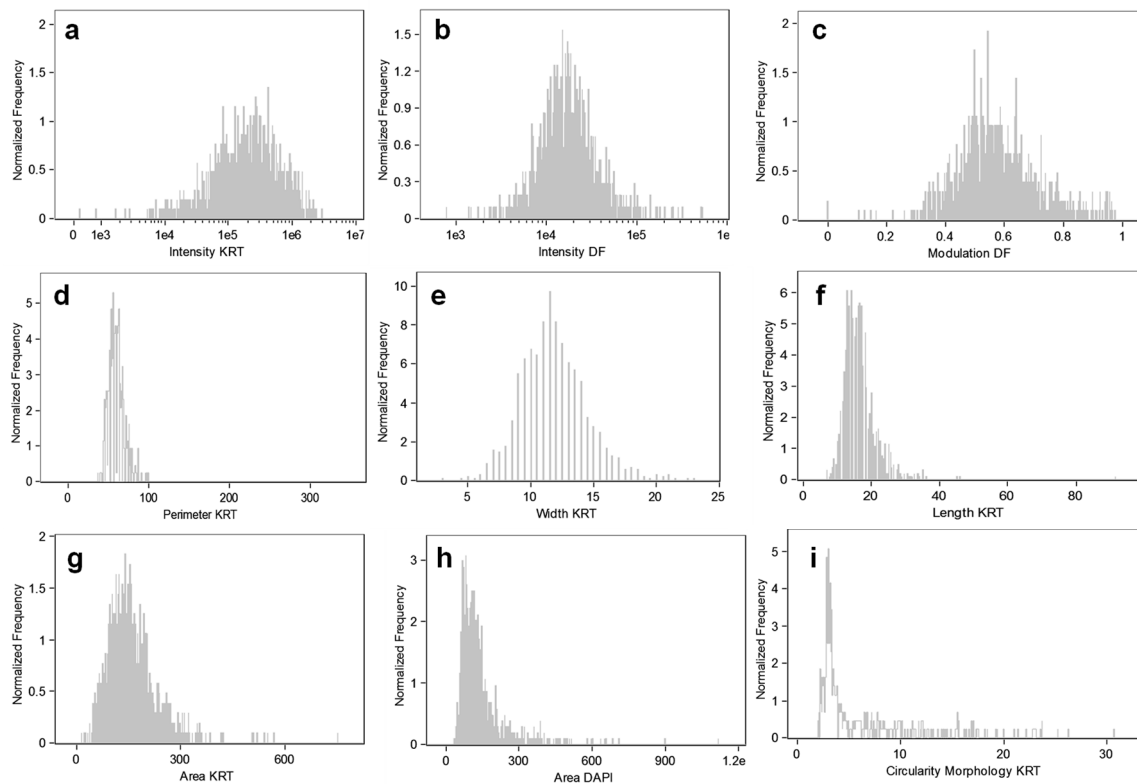


Figure 4. Histograms of Patient 1 Cytokeratin intensity (KRT) of the metastatic tumor cells (KRT positive, CD45 negative) (a), intensity of darkfield (b), modulation of darkfield (c), normalized intensity use to characterize contrast and texture in cells, calculated based on $\frac{\max \text{ pixel} - \min \text{ pixel}}{\max \text{ pixel} + \min \text{ pixel}}$, perimeter of KRT (d), width of KRT (e), length of KRT (f), area of KRT (g), area of DAPI (h) and circularity of KRT (i).

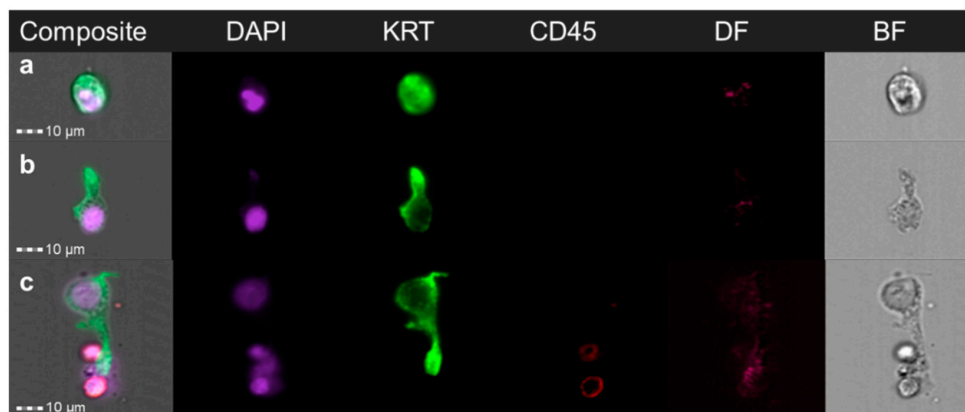


Figure 5. Malignant round Cytokeratin (KRT) positive cell (a), and elongated KRT positive cell (b,c) from Patient 1. Double positive KRT CD45 event containing three cells, two WBC and one elongated KRT positive cell (c).

A lymph node from a gall bladder cancer patient with multiple benign lymph nodes (Patient 3) was obtained and positive KRT staining cells were identified. However, there were no statistical cytological differences with malignant epithelial cells (Patient 1) (Figure 6) in cellular darkfield (intensity and darkfield modulation), or cellular morphology (Cytokeratin area). However, there was a slight shift in the cellular darkfield intensity for the benign sample compared to the malignant one implying greater granularity of these cells. Further studies are warranted to determine whether the observed difference in darkfield intensity could be used to discriminate between malignant and benign epithelial cells within lymph nodes.

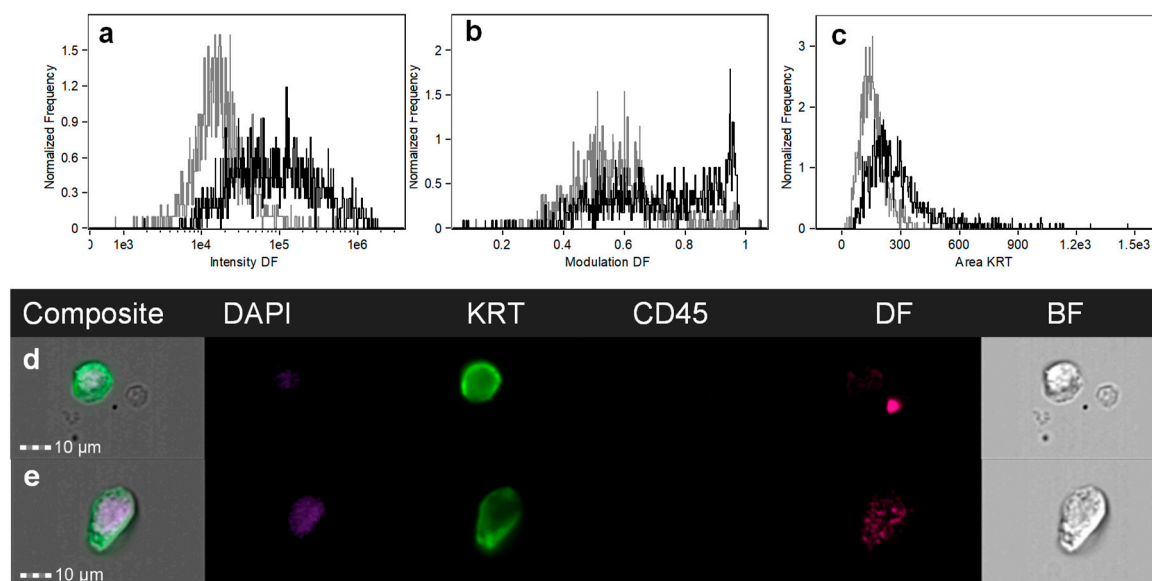


Figure 6. Histograms from cancerous and benign epithelial cells for intensity of darkfield (DF) (a), Modulation of DF (b) or Cytokeratin (KRT) area (c) between tumor cells (light grey) and benign (black) epithelial cells. Example of a benign round KRT positive cell (d), and benign KRT positive cell classified as elongated (e) from Patient 3.

4. Discussion

The presence of lymph node metastasis is an important adverse prognostic indicator for most types of solid cancers including GI malignancies. In the present study, a protocol was optimized for the recovery of epithelial tumor cells from lymph node tissues and combined with immunostaining and IFC towards the detection and cytomorphological characterization of metastatic cancer cells in GI cancer patient lymph nodes.

Using a cancer spiking model, we first demonstrated the feasibility of high throughput imaging of cancer cells present within a large lymphoid population (>100,000 cells). IFC provided high quality images of the tumor cells and enabled simultaneous immuno- and cytomorphological characterization to be conducted. Next, when assessing the sensitivity of this approach, we determined it was possible to detect cancer cells spiked in lymph nodes from a population of as little as 500 cancer cells. Such a sensitivity of detection, if translated to clinical samples, could be sufficient to detect the smallest micrometastasis of 0.2 mm which will have approximately 1000 tumor cells in three dimensions [1] or potentially even ITC. We note; however, this simplistic model does not mimic the complexity of a disseminated tumor and the cellular loss during sample preparation might differ significantly. Double negative (CD45⁻, KRT⁻) events were also identified and are likely to be non-lymphoid stromal lymph node cells (Figure 3b). These double negative events may also be due to sample degradation (including CD45 downregulation), due to a delay in sample processing.

Although no quantitative study could be carried out to determine the recovery yield of real tumor deposits within lymph nodes, we successfully applied the optimized protocol to analyze a positive

lymph node resected from a patient with advanced stomach adenocarcinoma. This confirmed the feasibility of using IFC to not only detect metastatic tumor cells in regional lymph nodes, but also to obtain detailed cytomorphological information about the tumor cells. While more extensive studies are required before drawing any conclusions about the diagnostic utility of this approach, this data illustrates the advantage of IFC for the analysis of resected specimens such as lymph nodes, as it provides a multitude of cytomorphological characteristics which cannot be obtained with standard flow cytometry. In addition, in the presence of minor incomplete tissue dissociation (i.e., presence of small clumps), which is a common occurrence, IFC is also effectively able to clarify double positive events (Figure 3e), i.e., events positive for both CD45 and KRT. Similar to advanced flow cytometry approaches, this is extremely advantageous as these double positive events can be discriminated and included in the analysis. In this study, cytomorphological analysis based solely on KRT staining could also provide valuable information. Indeed, the main advantage of IFC over other flow cytometry-based approaches is the multitude of cytomorphological information which is provided in a relatively high throughput (compared to microscopy scanning approaches including confocal microscopy). As discussed by Henning et al., current flow cytometry instruments can measure 30–40 parameters per event while the number of parameters that can be obtained from image-based approaches such as IFC are almost infinite [28].

Detection of cancer cells in lymph node tissues, especially micrometastasis and ITC, is highly dependent on the tissue processing and analysis technique [11]. In principle, dissociation and analysis of whole lymph nodes is more likely to eliminate sampling error and, therefore, accurately determine the total tumor load within resected tissue. In comparison, the gold standard histological examination of FFPE lymph node tissue, even combined with IHC, may result in a false negative result as small tumor deposits or ITCs may not be included in the examined sections [11]. A previous study by Ito and colleagues demonstrated the feasibility of intraoperative detection of tumor cells in lymph node tissue with flow cytometry in patients with non-small cell lung cancer that could be carried out within 40 min [29]. Similarly, Leers and colleagues have shown that multiparameter flow cytometry is useful for the detection of micrometastasis in SLN of breast cancer patients [30] and Hartana et al. in renal tumors [31]. More recently, Häyry and colleagues have shown that rapid nodal staging of head and neck cancer could be achieved with flow cytometry, demonstrating the fast and inexpensive nature of this new perioperative staging method [32]. Jagric and colleagues have demonstrated that for high risk SLN from gastric cancer patients, flow cytometry is highly specific in cancer detection although should not be used as a stand-alone method intra-operatively due to low sensitivity [33]. These approaches could be adapted for use with IFC providing both speed and morphological characterization. However, the inherently time and resource intensive nature of particularly imaging flow cytometry is a limitation as a routine intra-operative staging procedure.

Beyond simple detection of tumor cells, the main objective of this study was to demonstrate that detailed cytomorphological characterization of these cells can be readily obtained following their isolation. Rather than assessing tissue morphology or cellular morphology in a tissue context, we wanted to explore the concept of individual cancer cell morphology from dissociated lymph node tissue. In CTCs individual cellular morphology and its association with outcome has been investigated [17–21]. To our knowledge, this is the first time IFC has been used in the individual morphological characterization of cancer cells derived from lymph nodes.

To validate our approach, a lymph node with histologically confirmed metastatic tumor deposit was analyzed and compared to a control negative node. A large number of tumor cells could be readily identified and distinguished from lymphoid cells as they were pleomorphic. Cellular pleomorphism including spindle and round morphology as well as cell size has been associated with recurrence risk [34] and poorer patient outcome [35]. For example, epithelial to mesenchymal transition (EMT) is an important biological process resulting in cytomorphological and phenotypical changes with poorer outcomes when identified in CTCs [35]. Importantly, evidence suggests metastasis via lymphatics does

not always require EMT [15] and so further morphological analysis of tumor cells in lymph nodes is warranted.

The relevance of morphological changes varies drastically depending on the tissue of origin and environmental stressors. For example, comparison of two cell lines, SW480 derived from primary colorectal cancer and SW620 derived from a lymph node metastasis, showed mostly spreading epithelial morphology with rough surface/protrusions or ovoid morphology with a smoother membrane, respectively [36]. Specifically in the primary tumor, elongated cells have a greater ability to metastasize spontaneously than rounded cells, while in the lymph node rounded cells are more likely to undergo metastasis [36]. However, it is difficult to characterize the morphologies of individual cells based on conventional histology sections as the dissection plane may alter observation of the cells of interest. 3D modeling and serial sectioning have been performed in an attempt to overcome this issue [37]. Research investigating changes in individual morphologies of dissociated cells particularly tumor cells from lymph nodes may provide some insights.

Comparison of the primary tumor tissue with lymph node metastasis can identify important markers in invasion [38–40], potentially analyzing other metastatic sites and cellular phenotypes/morphology may offer further insights. The current study demonstrates that IFC is an ideal technology to carry out such studies. IFC may also prove useful to evaluate expression of additional markers (e.g., stem cell CD133, CD44 [38], mesenchymal, or other markers including AFAP1L1 [41]) which in combination with individual morphological characterization could potentially allow for the selection of personalized treatments. This technique could also be applied to the analysis of DTC in bone marrow for which morphological and phenotypical analysis could be extremely advantageous for improving risk prevention and tailored treatment [42]. However, conventional flow cytometry has a lower sensitivity than other methods and there have been few studies conducted on large patient cohorts [42].

Similar to immunomagnetic bead separation, the current study is still reliant on cellular phenotype for detection [42] and therefore may bias analysis in the case of marker down regulation. Another limitation of the proposed approach and others that use immuno-based and molecular approaches is that rare benign epithelial inclusions [43] or hematological cells expressing epithelial antigens [44], potentially due to phagocytized KRT debris [45], can lead to false positive results. These events are extremely rare and while the exact prevalence rate is unknown, one breast cancer study reported false positives due to ectopic breast tissue in SLNs occurring in seven cases out of >35,000 cases (<0.2%) [46]. It is important to be able to accurately distinguish inclusions from true metastatic depositions in order to achieve accurate staging [47]. Differentiation between benign epithelial inclusions and metastatic deposits in solid tumors is currently best achieved using standard histological criteria with assistance of IHC but this distinction in some cases may be extremely difficult and the use of molecular techniques without histological verification may lead to over-diagnosis [48]. Although it is stated that in the semi-quantitative One-Step-Nucleic-Acid Amplification (OSNA) approach benign epithelial inclusions will not necessarily produce a false positive result, as often the epithelial positive threshold is not reached [48].

To investigate the possibility of false positives due to benign inclusions, we obtained a lymph node from a gall bladder cancer patient (Patient 3). As in Patient 1 (cancer positive node), we also found positive KRT staining cells in this sample, which would produce a false positive result in a clinical setting. We were unable to accurately distinguish benign and malignant epithelial cells based on differences in cellular darkfield (intensity and darkfield modulation) in these two samples. However, we did note a small difference in darkfield intensity which warrants further investigation. Additional samples may also help us to distinguish morphological differences. Conventional morphological differences (nucleus area) was also not a distinguishing factor in this semi-automated analysis and the lack of difference was potentially compounded by the cells being in suspension rather than attached flat to a slide. As noted above, the incorporation of immunomarkers more specific to tumor cells should, therefore, be used to unambiguously eliminate the risk of false-positives associated to the presence of benign lesions. Moreover, the use of IFC to define and explore nucleus to cytoplasm ratio in additional samples may provide further insight, particularly when differentiating benign from malignant cancer cells.

5. Conclusions

We have successfully demonstrated for the first time the feasibility of using IFC for the detection, enumeration, and characterization of tumor cancer cells disseminated in gastrointestinal cancer patient lymph nodes. When used in addition to conventional histological techniques, IFC may offer extra phenotypical and cytomorphological information regarding disease progression as it provides the statistical significance of analyzing thousands of cells in a short period of time. This IFC approach assists in better determining patient prognosis and therefore in personalizing treatment regimens, as the presence of tumor cells with specific cytomorphological features may indicate that a more aggressive treatment is warranted.

Supplementary Materials: Supplementary materials can be found at <http://www.mdpi.com/2624-5647/1/4/30/s1>.

Author Contributions: Conceptualization, M.W. and B.T.; methodology, M.W., R.G., and A.R.; software, M.W.; validation, M.W.; formal analysis, M.W., R.G., and B.T.; investigation, M.W. and B.T.; resources, R.G., A.R., and B.T.; data curation, M.W. and B.T.; writing—original draft preparation, M.W., R.G., and B.T.; writing—review and editing, M.W., B.T., R.G., and A.R.; supervision, B.T. and R.G.; project administration, M.W. and B.T.; funding acquisition B.T.

Funding: This research was supported by the ARC Centre of Excellence in Convergent Bio-Nano Science and Technology and the NHMRC under grant [APP1045841].

Acknowledgments: The authors would like to thank Teresa Tin for her expert technical assistance. The authors would also like to acknowledge and thank the patients involved in this study.

Conflicts of Interest: None of the authors declare any potential conflicts of interest including competing financial interests at the time of submission.

References

1. Edge, S.; Byrd, D.; Compton, C.; Fritz, A.; Greene, F.; Trotti, A., III. *AJCC Cancer Staging Manual*, 7th ed.; Springer: New York, NY, USA, 2010.
2. Estrada, O.; Pulido, L.; Admella, C.; Hidalgo, L.-A.; Clavé, P.; Sunol, X. Sentinel lymph node biopsy as a prognostic factor in non-metastatic colon cancer: A prospective study. *Clin. Transl. Oncol.* **2016**, *19*, 432–439. [[CrossRef](#)] [[PubMed](#)]
3. Arigami, T.; Uenosono, Y.; Yanagita, S.; Nakajo, A.; Ishigami, S.; Okumura, H.; Kijima, Y.; Ueno, S.; Natsugoe, S. Clinical significance of lymph node micrometastasis in gastric cancer. *Ann. Surg. Oncol.* **2012**, *20*, 515–521. [[CrossRef](#)] [[PubMed](#)]
4. Chen, S.L.; Hoehne, F.M.; Giuliano, A.E. The prognostic significance of micrometastases in breast cancer: A seer population-based analysis. *Ann. Surg. Oncol.* **2007**, *14*, 3378–3384. [[CrossRef](#)] [[PubMed](#)]
5. Patani, N.; Mokbel, K. Clinical significance of sentinel lymph node isolated tumour cells in breast cancer. *Breast Cancer Res. Treat.* **2011**, *127*, 325–334. [[CrossRef](#)] [[PubMed](#)]
6. Wu, Y.; Mittendorf, E.A.; Kelten, C.; Tucker, S.L.; Wei, W.; Middleton, L.P.; Broglio, K.; Buchholz, T.A.; Hunt, K.K.; Sahin, A.A. Occult axillary lymph node metastasis do not have prognostic significance in early stage breast cancer. *Cancer* **2011**, *118*, 1507–1514. [[CrossRef](#)] [[PubMed](#)]
7. Murali, R.; DeSilva, C.; McCarthy, S.W.; Thompson, J.F.; Scolyer, R.A. Sentinel lymph nodes containing very small (<0.1 mm) deposits of metastatic melanoma cannot be safely regarded as tumor-negative. *Ann. Surg. Oncol.* **2012**, *19*, 1089–1099. [[PubMed](#)]
8. Naidoo, K.; Pinder, S.E. Micro-and macro-metastasis in the axillary lymph node: A review. *Surgeon* **2016**, *15*, 76–82. [[CrossRef](#)] [[PubMed](#)]
9. Giuliano, A.E.; McCall, L.; Beitsch, P.; Whitworth, P.W.; Blumencranz, P.; Leitch, A.M.; Saha, S.; Hunt, K.K.; Morrow, M.; Ballman, K. Locoregional recurrence after sentinel lymph node dissection with or without axillary dissection in patients with sentinel lymph node metastases: The american college of surgeons oncology group z0011 randomized trial. *Ann. Surg.* **2010**, *252*, 426–433. [[CrossRef](#)]
10. Briganti, A.; Passoni, N.M.; Abdollah, F.; Nini, A.; Montorsi, F.; Karnes, R.J. Treatment of lymph node-positive prostate cancer: Teaching old dogmas new tricks. *Eur. Urol.* **2014**, *65*, 26–28. [[CrossRef](#)] [[PubMed](#)]
11. Winter, M.; Gibson, R.; Ruszkiewicz, A.; Thompson, S.K.; Thierry, B. Beyond conventional pathology: Towards preoperative and intraoperative lymph node staging. *Int. J. Cancer* **2015**, *136*, 743–751. [[CrossRef](#)]

12. Grabau, D.; Ryden, L.; Fernö, M.; Ingvar, C. Analysis of sentinel node biopsy—A single-institution experience supporting the use of serial sectioning and immunohistochemistry for detection of micrometastases by comparing four different histopathological laboratory protocols. *Histopathology* **2011**, *59*, 129–138. [[CrossRef](#)] [[PubMed](#)]
13. Cristofanilli, M.; Hayes, D.F.; Budd, G.T.; Ellis, M.J.; Stopeck, A.; Reuben, J.M.; Doyle, G.V.; Matera, J.; Allard, W.J.; Miller, M.C. Circulating tumor cells: A novel prognostic factor for newly diagnosed metastatic breast cancer. *J. Clin. Oncol.* **2005**, *23*, 1420–1430. [[CrossRef](#)] [[PubMed](#)]
14. Pilati, P.; Mocellin, S.; Bertazza, L.; Galdi, F.; Briarava, M.; Mammano, E.; Tessari, E.; Zavagno, G.; Nitti, D. Prognostic value of putative circulating cancer stem cells in patients undergoing hepatic resection for colorectal liver metastasis. *Ann. Surg. Oncol.* **2012**, *19*, 402–408. [[CrossRef](#)] [[PubMed](#)]
15. Banyard, J.; Bielenberg, D.R. The role of emt and met in cancer dissemination. *Connect. Tissue Res.* **2015**, *56*, 403–413. [[CrossRef](#)] [[PubMed](#)]
16. Haber, D.A.; Velculescu, V.E. Blood-based analyses of cancer: Circulating tumor cells and circulating tumor DNA. *Cancer Discov.* **2014**, *4*, 650–661. [[CrossRef](#)]
17. Lighthart, S.T.; Coumans, F.A.; Bidard, F.-C.; Simkens, L.H.; Punt, C.J.; de Groot, M.R.; Attard, G.; de Bono, J.S.; Pierga, J.-Y.; Terstappen, L.W. Circulating tumor cells count and morphological features in breast, colorectal and prostate cancer. *PLoS ONE* **2013**, *8*, e67148. [[CrossRef](#)]
18. Marrinucci, D.; Bethel, K.; Bruce, R.H.; Curry, D.N.; Hsieh, B.; Humphrey, M.; Krivacic, R.T.; Kroener, J.; Kroener, L.; Ladanyi, A. Case study of the morphologic variation of circulating tumor cells. *Hum. Pathol.* **2007**, *38*, 514–519. [[CrossRef](#)] [[PubMed](#)]
19. Marrinucci, D.; Bethel, K.; Lazar, D.; Fisher, J.; Huynh, E.; Clark, P.; Bruce, R.; Nieva, J.; Kuhn, P. Cytomorphology of circulating colorectal tumor cells: A small case series. *J. Oncol.* **2010**, *2010*, 861341. [[CrossRef](#)]
20. Park, S.; Ang, R.R.; Duffy, S.P.; Bazov, J.; Chi, K.N.; Black, P.C.; Ma, H. Morphological differences between circulating tumor cells from prostate cancer patients and cultured prostate cancer cells. *PLoS ONE* **2014**, *9*, e85264. [[CrossRef](#)]
21. Vona, G.; Estepa, L.; Bérout, C.; Damotte, D.; Capron, F.; Nalpas, B.; Mineur, A.; Franco, D.; Lacour, B.; Pol, S. Impact of cytomorphological detection of circulating tumor cells in patients with liver cancer. *Hepatology* **2004**, *39*, 792–797. [[CrossRef](#)]
22. Headland, S.E.; Jones, H.R.; D'Sa, A.S.; Perretti, M.; Norling, L.V. Cutting-edge analysis of extracellular microparticles using imagestreamx imaging flow cytometry. *Sci. Rep.* **2014**, *4*, 5237. [[CrossRef](#)] [[PubMed](#)]
23. Basiji, D.; O'Gorman, M. Imaging flow cytometry. *J. Immunol. Methods* **2015**, *423*, 1–2. [[CrossRef](#)] [[PubMed](#)]
24. Goda, K.; Ayazi, A.; Gossett, D.R.; Sadasivam, J.; Lonappan, C.K.; Sollier, E.; Fard, A.M.; Hur, S.C.; Adam, J.; Murray, C. High-throughput single-microparticle imaging flow analyzer. *Proc. Natl. Acad. Sci. USA* **2012**, *109*, 11630–11635. [[CrossRef](#)] [[PubMed](#)]
25. Reyes, E.E.; VanderWeele, D.J.; Isikbay, M.; Duggan, R.; Campanile, A.; Stadler, W.M.; Vander Griend, D.J.; Szmulewitz, R.Z. Quantitative characterization of androgen receptor protein expression and cellular localization in circulating tumor cells from patients with metastatic castration-resistant prostate cancer. *J. Transl. Med.* **2014**, *12*, 313. [[CrossRef](#)] [[PubMed](#)]
26. Doan, M.; Vorobjev, I.; Rees, P.; Filby, A.; Wolkenhauer, O.; Goldfeld, A.E.; Lieberman, J.; Barteneva, N.; Carpenter, A.E.; Hennig, H. Diagnostic potential of imaging flow cytometry. *Trends Biotechnol.* **2018**, *36*, 649–652. [[CrossRef](#)] [[PubMed](#)]
27. Liu, T.; Winter, M.; Thierry, B. Quasi-spherical microwells on superhydrophobic substrates for long term culture of multicellular spheroids and high throughput assays. *Biomaterials* **2014**, *35*, 6060–6068. [[CrossRef](#)]
28. Hennig, H.; Rees, P.; Blasi, T.; Kamentsky, L.; Hung, J.; Dao, D.; Carpenter, A.E.; Filby, A. An open-source solution for advanced imaging flow cytometry data analysis using machine learning. *Methods* **2017**, *112*, 201–210. [[CrossRef](#)]
29. Ito, M.; Minamiya, Y.; Kawai, H.; Saito, S.; Saito, H.; Imai, K.; Ogawa, J.-I. Intraoperative detection of lymph node micrometastasis with flow cytometry in non-small cell lung cancer. *J. Thorac. Cardiovasc. Surg.* **2005**, *130*, 753–758. [[CrossRef](#)]
30. Leers, M.; Schoffelen, R.; Hoop, J.; Theunissen, P.; Oosterhuis, J.; Rahmy, A.; Tan, W.; Nap, M. Multiparameter flow cytometry as a tool for the detection of micrometastatic tumour cells in the sentinel lymph node procedure of patients with breast cancer. *J. Clin. Pathol.* **2002**, *55*, 359–366. [[CrossRef](#)]

31. Hartana, C.A.; Kinn, J.; Rosenblatt, R.; Anania, S.; Alamdari, F.; Glise, H.; Sherif, A.; Winqvist, O. Detection of micrometastases by flow cytometry in sentinel lymph nodes from patients with renal tumours. *Br. J. Cancer* **2016**, *115*, 957–966. [[CrossRef](#)]
32. Häyry, V.; Kågedal, Å.; Hjalmarsson, E.; da Silva, P.F.N.; Drakskog, C.; Margolin, G.; Georén, S.K.; Munck-Wikland, E.; Winqvist, O.; Cardell, L.O. Rapid nodal staging of head and neck cancer surgical specimens with flow cytometric analysis. *Br. J. Cancer* **2018**, *118*, 421–427. [[CrossRef](#)] [[PubMed](#)]
33. Jagric, T.; Mis, K.; Gorenjak, M.; Goropevsek, A.; Kavalari, R.; Mars, T. Can flow cytometry reinvent the sentinel lymph node concept in gastric cancer patients? *J. Surg. Res.* **2018**, *223*, 46–57. [[CrossRef](#)] [[PubMed](#)]
34. Friedl, P.; Wolf, K. Tumour-cell invasion and migration: Diversity and escape mechanisms. *Nat. Rev. Cancer* **2003**, *3*, 362–374. [[CrossRef](#)]
35. Kevans, D.; Wang, L.M.; Sheahan, K.; Hyland, J.; O'Donoghue, D.; Mulcahy, H.; O'Sullivan, J. Epithelial-mesenchymal transition (emt) protein expression in a cohort of stage ii colorectal cancer patients with characterized tumor budding and mismatch repair protein status. *Int. J. Surg. Pathol.* **2011**, *19*, 751–760. [[CrossRef](#)] [[PubMed](#)]
36. Palmieri, V.; Lucchetti, D.; Maiorana, A.; Papi, M.; Maulucci, G.; Calapà, F.; Ciasca, G.; Giordano, R.; Sgambato, A.; De Spirito, M. Mechanical and structural comparison between primary tumor and lymph node metastases cells in colorectal cancer. *Soft Matter* **2015**, *11*, 5719–5726. [[CrossRef](#)] [[PubMed](#)]
37. Margheri, F.; Luciani, C.; Taddei, M.L.; Giannoni, E.; Laurenzana, A.; Biagioni, A.; Chilla, A.; Chiarugi, P.; Fibbi, G.; Del Rosso, M. The receptor for urokinase-plasminogen activator (upar) controls plasticity of cancer cell movement in mesenchymal and amoeboid migration style. *Oncotarget* **2014**, *5*, 1538–1553. [[CrossRef](#)]
38. Wakamatsu, Y.; Sakamoto, N.; Oo, H.Z.; Naito, Y.; Uraoka, N.; Anami, K.; Sentani, K.; Oue, N.; Yasui, W. Expression of cancer stem cell markers aldh1, cd44 and cd133 in primary tumor and lymph node metastasis of gastric cancer. *Pathol. Int.* **2012**, *62*, 112–119. [[CrossRef](#)] [[PubMed](#)]
39. Takes, R.P.; de Jong, B.; Robert, J.; Wijffels, K.; Schuurin, E.; Litvinov, S.V.; Hermans, J.; van Krieken, H.J. Expression of genetic markers in lymph node metastases compared with their primary tumours in head and neck cancer. *J. Pathol.* **2001**, *194*, 298–302. [[CrossRef](#)]
40. Nishizaki, T.; DeVries, S.; Chew, K.; Goodson, W.H.; Ljung, B.-M.; Thor, A.; Waldman, F.M. Genetic alterations in primary breast cancers and their metastases: Direct comparison using modified comparative genomic hybridization. *Genes Chromosomes Cancer* **1997**, *19*, 267–272. [[CrossRef](#)]
41. Takahashi, R.; Nagayama, S.; Furu, M.; Kajita, Y.; Jin, Y.; Kato, T.; Imoto, S.; Sakai, Y.; Toguchida, J. Afap111, a novel associating partner with vinculin, modulates cellular morphology and motility, and promotes the progression of colorectal cancers. *Cancer Med.* **2014**, *3*, 759–774. [[CrossRef](#)]
42. Riethdorf, S.; Wikman, H.; Pantel, K. Review: Biological relevance of disseminated tumor cells in cancer patients. *Int. J. Cancer* **2008**, *123*, 1991–2006. [[CrossRef](#)] [[PubMed](#)]
43. Resetkova, E.; Hoda, S.A.; Clarke, J.L.; Rosen, P.P. Benign heterotopic epithelial inclusions in axillary lymph nodes. *Arch. Pathol. Lab. Med.* **2003**, *127*, e25–e27. [[PubMed](#)]
44. Dunphy, C.H. Pitfalls of frozen section to intraoperative consultations of evaluating lymph nodes for involvement by metastatic malignancies: Benign processes mimicking metastatic carcinoma. In *Frozen Section Library: Lymph Nodes*; Springer: Berlin/Heidelberg, Germany, 2012; pp. 95–119.
45. Rao, R.S.; Taylor, J.; Palmer, J.; Jennings, W.C. Breast cancer pseudometastasis in a sentinel lymph node with cytokeratin-positive debris. *Breast J.* **2005**, *11*, 134–137. [[CrossRef](#)] [[PubMed](#)]
46. Maiorano, E.; Mazzarol, G.M.; Pruneri, G.; Mastropasqua, M.G.; Zurrida, S.; Orvieto, E.; Viale, G. Ectopic breast tissue as a possible cause of false-positive axillary sentinel lymph node biopsies. *Am. J. Surg. Pathol.* **2003**, *27*, 513–518. [[CrossRef](#)] [[PubMed](#)]
47. Fellegara, G.; Carcangiu, M.L.; Rosai, J. Benign epithelial inclusions in axillary lymph nodes: Report of 18 cases and review of the literature. *Am. J. Surg. Pathol.* **2011**, *35*, 1123–1133. [[CrossRef](#)] [[PubMed](#)]
48. Bernet, L.; Cano, R.; Martinez, M.; Dueñas, B.; Matias-Guiu, X.; Morell, L.; Palacios, J.; Rezola, R.; Robles-Frias, M.; Ruiz, I. Diagnosis of the sentinel lymph node in breast cancer: A reproducible molecular method: A multicentric spanish study. *Histopathology* **2011**, *58*, 863–869. [[CrossRef](#)]

